Int. J. Heat Mass Transfer. Vol. 18, pp. 1397–1407. Pergamon Press 1975. Printed in Great Britain

OPTICAL AND ELECTROCHEMICAL STUDIES OF TRANSIENT FREE CONVECTION MASS TRANSFER AT HORIZONTAL SURFACES

M. A. PATRICK and A. A. WRAGG
Department of Chemical Engineering, University of Exeter, Exeter, Devon, U.K.

(*Received* 25 *November* 1974 *and in revised form* 22 *January* 1975)

Abstract—The onset of free convection at upward facing horizontal surfaces adjacent to a free fluid environment has been studied using the electrochemical system involving the electrodeposition of Cu^{2+} ions. A transient potential step technique was employed and photography of the ensuing developing convective structure was synchronised with the recording of current–time transients. This enabled the interdependence of instantaneous mass-transfer rate and convective flow structure to be visualised. A number of distinctive flow structures in the transient and steady states were observed and these have been related to the correlation regimes for the overall mass-transfer rate. Interesting phenomena involving periodic instabilities have been discovered at transitional Rayleigh numbers leading to pulsations in the convective plume and corresponding regular oscillations in the steady state mass-transfer rate.

The effect of surface roughening on mass transfer and hydrodynamic performance during extended experiments has been observed and a method of overcoming surface roughening difficulties in the application of the electrochemical technique is suggested.

Diffusion transient undershoot times are correlated in terms of plate Rayleigh number by the equations

$$\frac{Dt}{d^2} = 32{\cdot}5(Gr_d Sc)^{-2/3}$$

in the range $10^7 < Re_d < 10^{11}$ and

$$\frac{Dt}{d^2} = 1{\cdot}80(Gr_d Sc)^{-0{\cdot}51}$$

in the range $10^4 < Ra_d < 10^7$.

The periodic fluctuation frequencies are similarly correlated by the equation

$$\frac{Dt}{d^2} = 12{\cdot}8(Gr_d Sc)^{-2/3}.$$

NOMENCLATURE

- A, electrode surface area;
- c, molar concentration of reacting ions;
- D, ionic diffusion coefficient;
- d, diameter of electrode surface;
- F, Faraday number (96 500 C Mol^{-1});
- Gr, Grashof number;
- g, gravitational acceleration;
- i_L, limiting electrolysis current;
- k_m, mean mass-transfer coefficient;
- Nu, Nusselt number;
- Ra, Rayleigh number, $Sc \times Gr$;
- Sc, Schmidt number;
- Sh, Sherwood number;
- t, time;
- y, distance normal to electrode surface;
- z, reaction valency.

Greek symbols

- δ, diffusion layer thickness;
- γ, densification coefficient;
- ν, kinematic viscosity of fluid;
- ρ, density of fluid;
- $\Delta\rho$, density difference between interface and bulk.

Subscripts

- ∞, refers to bulk concentration;
- 0, refers to interfacial conditions;
- u, refers to undershoot;
- b, refers to diffusion layer breakup.

INTRODUCTION

THIS paper describes an experimental study of phenomena occurring during the onset of free convection above plane horizontal surfaces in fluid–solid mass transfer. The electrochemical technique of mass-transfer measurement (e.g. [1–3]) has been employed as this allows precise monitoring of the instantaneous transfer rate as a function of time. Schlieren photographs of the observed convection have been synchronized with the current recordings in order to observe the interdependence of the mass-transfer rate and the hydrodynamic structure above the electrode surfaces.

In previous work with a similar system steady state free convective mass-transfer rates were measured and successfully correlated for a wide range of experimental conditions [4]. Further work involving a simple shadowgraph technique illustrated the variety of convective flow types possible in steady state conditions [5].

The problem under discussion is analogous to cases of heat transfer from heated surfaces into unrestricted fluids and certain previous papers on this topic are directly relevant. For instance Soehngen [6] undertook an extensive investigation of the transient performance of heated cylinders in high Prandtl number fluids. For different heating rates the value of the thermal boundary-layer thickness and Nusselt number were measured with time. A pronounced overshoot of the boundary-layer thickness was noted with respect to the final steady state value with a corresponding undershoot of the heat-transfer coefficient. Vest and Lawson [7] have studied the onset of convection adjacent to a suddenly heated horizontal wire, the development of the temperature field and its subsequent distortion upon convection onset being observed by Mach–Zender interferometry. Optical studies of convection above plane heated surfaces of various geometries were described by Husar and Sparrow [8] and more recently Sparrow, Husar and Goldstein [9] have investigated the generation of thermals at a horizontal surface and have measured the periodic fluctuation of local temperature above an active thermal-generating site.

There appears to be no previous detailed work on the onset of convection in mass-transfer systems and no previous attempt in either heat or mass transfer to explore the interesting region between the end of the transient diffusion (or conduction) period and the steady state free convection period, in terms of the dependence of the instantaneous heat- or mass-transfer rate on the developing flow structure. The present study was therefore undertaken in order to elucidate some of these phenomena and also in order to obtain clearer and more instructive photographs of steady state free convection than those provided by [5].

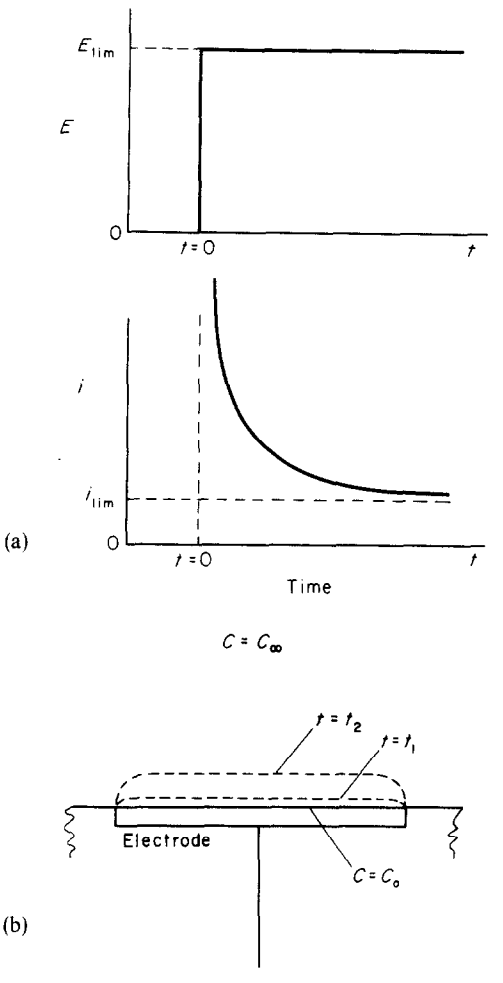

FIG. 1(a). Potential step and transient current response. (b) Boundary conditions and diffusion layer growth at the solid–liquid interface.

THEORETICAL DISCUSSION

The electrochemical technique has become a widely accepted method of mass-transfer measurement and heat-transfer modelling due to its convenience and precision. In the present work the process used was the cathodic electrodeposition of Cu^{2+} ions from a swamping 1·5M sulphuric acid electrolyte the presence of which effectively eliminates migration transport of Cu^{2+} and ensures diffusion–convection control. Operation at limiting electrolysis current facilitates calculation of the mass-transfer coefficient from the measured current and bulk concentration of transferring species through the simple equation

$$k_m = \frac{i_L}{zFAc_\infty} \tag{1}$$

since the interfacial concentration approaches zero. The basis of the present experimental approach was the sudden switch-on to the active cathode surfaces of a potential corresponding to the limiting current so that the interfacial Cu^{2+} concentration was suddenly constrained to a value of zero. The response of the current was then monitored with time and its gradual fall from a theoretically infinite initial value due to the gradual build up of the diffusion layer was observed. The potential and current variation with time is illustrated in Fig. 1(a) and the conditions at the electrode are depicted in Fig. 1(b).

The shape of the current–time transient corresponding to a simple diffusion process in the fluid adjacent to the plate surface is easily predicted from the solution of the one-dimensional unsteady-state diffusion equation, with surface concentration of c_0 for $t \geqslant 0$. From this the mass-transfer rate and hence current may be expressed as a function of time, the equation for the Cu^{2+} system becoming

$$\frac{i}{A} = 1{\cdot}08 \times 10^5 c_\infty \left\{\frac{D}{t}\right\}^{1/2}. \tag{2}$$

Such transient techniques are common in electrochemical science and may be used for instance for the measurement of ionic diffusion coefficients at suitably designed electrodes.

As the diffusion boundary layer adjacent to the electrode becomes progressively thicker an unstable situation arises due to the existence of a less dense layer of solution under the heavier bulk solution and

this leads eventually to the onset of convection and the attainment of a time–steady transfer rate. A critical value of the Rayleigh number, based on boundary-layer thickness as characteristic dimension, characterizes the limit of stability. For their analogous heat-transfer study Sparrow, Husar and Goldstein determined a critical Rayleigh number of approximately 1800.

Once convection has begun, a variety of flow structures are possible above a circular horizontal surface depending upon the surface dimensions and the physical properties of the fluid. At relatively small surfaces and with low Sc and Pr fluids a laminar boundary-layer flow occurs radially inwards feeding a single centrally ascending steady laminar plume. Rotem and Claassen [10, 11] are among authors who have theoretically analysed this case for heat transfer and they have presented [11] colour Schlieren pictures of boundary-layer flow on a plate and discussed the transition to instability. Some theoretical and experimental equations describing heat and mass transfer in horizontal boundary-layer flows have recently been compared in [12]. With relatively large surfaces, boundary layers thicken above the stability limit and in heat transfer the intermittent generation of thermals results at fixed sites, as discussed and photographed by Sparrow, Husar and Goldstein. Howard [13] has presented a phenomenological model by which the periodicity of thermal generation may be explained. The model is based on the concept of a conductive phase followed by a break-off and mixing phase in a periodic cycle. Since thermals are generated at a multiplicity of sites on the surface the overall time-averaged heat-transfer rate is independent of surface dimensions, though, of course, local fluctuation of heat flux and temperature field must occur. A similar behaviour would be anticipated in solid–liquid mass transfer though the high value of the Schmidt numbers would be expected to lead to close spaced mass convection streams.

At conditions intermediate between these extremes a transitional type of flow structure consisting of a periodically erupting plume was demonstrated in the earlier study [5], the range of $Gr_d Sc$ in which transition occurred being tentatively suggested as $3 \times 10^6 - 2 \times 10^8$.

Steady state mass-transfer rates were correlated [4, 5] by the equation

$$Sh = 0{\cdot}72(Gr_d . Sc)^{0{\cdot}25} \quad (3)$$

in the range $3 \times 10^4 < Gr_d . Sc < 3 \times 10^7$ and by

$$Sh = 0{\cdot}18(Gr_d . Sc)^{0{\cdot}33} \quad (4)$$

in the range $3 \times 10^7 < Gr_d . Sc < 10^{12}$.

No detailed study has yet been made of the interrelationship of instantaneous mass-transfer rate and flow structure during the actual onset of convection and it was the main purpose of the present study to elucidate this behaviour.

EXPERIMENTAL

Horizontal copper disk cathodes were flush mounted in perspex decks and fitted into the base of a glass sided rectangular tank. The copper plate anode was suspended from the lid. Cathodes of 1, 2·5, 10, 20 and 50 mm diameter were used. The cell was filled with electrolyte containing 1·5 M H_2SO_4 and a range of concentrations of Cu SO_4 were added, 0·005, 0·02, 0·05, 0·1, 0·3 M. The cell was positioned in a standard Toepler Schlieren optical system which facilitated the photography of any change in concentration of the solution above the electrodes. The electrical circuit consisted of a stabilized power unit, a high impedance voltmeter and a Y–t recorder which measured the current flowing in the circuit via the potential difference produced across a variable known resistance from a decade box. The essential details of the apparatus are shown in Fig. 2.

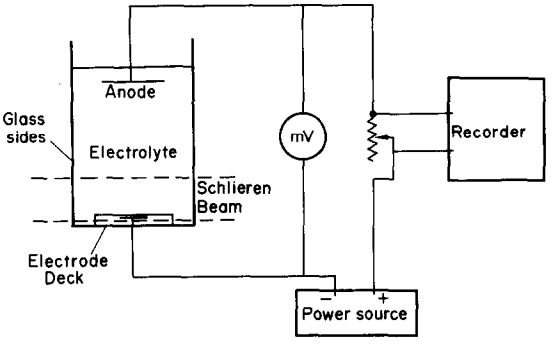

FIG. 2. Experimental cell and circuit.

Prior to each experiment the cathode surfaces were polished with fine emery cloth and washed. For each electrode/solution combination a standard current–potential curve was plotted in order to measure the limiting current and also to determine a suitable potential value corresponding to limiting current conditions. Current transients were then taken in homogeneous stagnant fluid conditions by sudden switch-on of the predetermined potential and monitoring of the current response as a function of time. As soon as convection became visible above the electrode, photography of the various stages of development of the flow structure was commenced. Where appropriate, the frequency of flow pulsation was measured by visual observation.

In conditions of strong electrolyte concentration certain experiments were prolonged in order to observe the effect of electrode roughening on mass-transfer rate and flow. In further experiments a series of successive potential steps were applied in order to observe the effect of progressive roughening on the shape of the transient. In these runs the electrode was active for 10 min and was then switched off for 10 min prior to a further potential step application.

RESULTS

The programme of work resulted in the systematic collection of several hundred photographs showing various stages of convection development for each combination of experimental variables. It has therefore been necessary to restrict the presentation here to

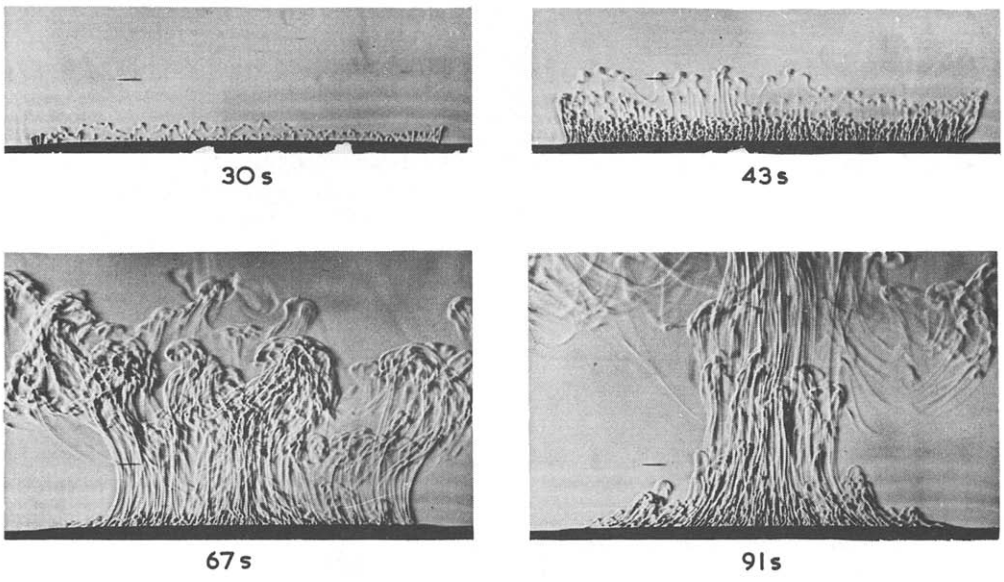

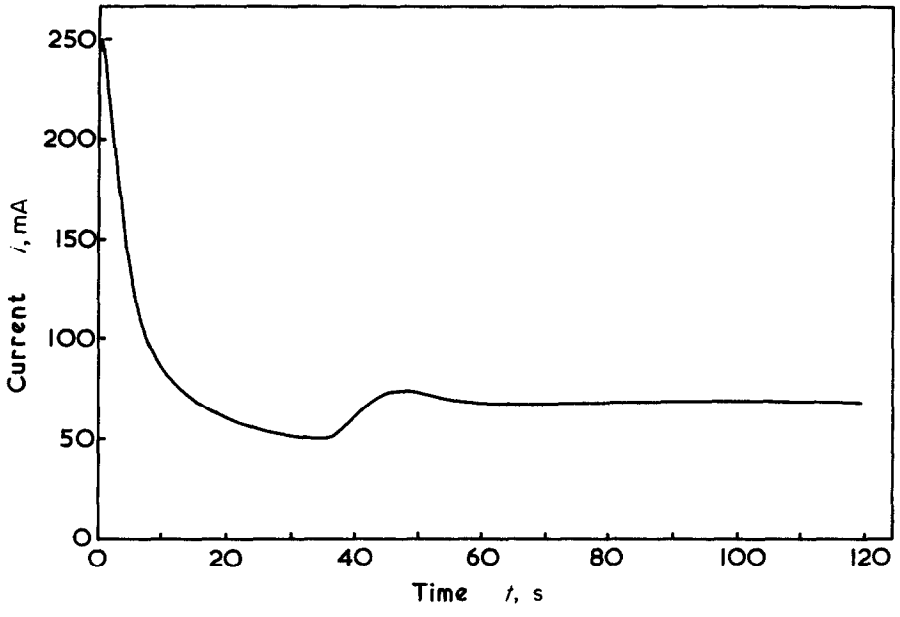

FIG. 3. Current–time plot and convection development for 50 mm electrode in 0·05 M solution, $Ra_d = 1{\cdot}35 \times 10^{10}$.

selected representative examples and in Figs. 3–6 four distinct cases are depicted. In each case the current vs time transient is plotted and the time of each photograph is indicated. In the calculation of the quoted *Gr* and *Ra* numbers the values of electrolyte viscosity and density were taken from Eisenberg *et al.* [14] and those of Cu^{2+} diffusivity from Arvia *et al.* [15]. The $\Delta\rho$ terms were calculated according to the procedure of Wilke *et al.* [16].

Figure 3 refers to the 50 mm electrode in the 0·05M solution. The transient is seen to undershoot and then overshoot the eventual steady limiting current value. It is notable that convection is distinctly visible before the undershoot minimum is reached at about, $t_u = 35$ seconds. The sharp increase in the mass-transfer rate is then caused by the first main generation of convection streams which may be seen to be well established at $t = 43$ s. Necking of the plume then occurs ($t = 67$ s) and the mass-transfer rate falls until a steady-state situation arises ($t = 91$ s), in which there is a complex flow structure consisting of a multiplicity of close spaced interacting convection streams.

The opposite extreme case of the onset of single plumed steady laminar convection is depicted in Fig. 4 for the case of the 1 mm electrode in 0·3M solution. Again a marked undershoot and overshoot is apparent in this case t_u being much shorter, approximately 5 s.

Figures 5 and 6 present two intermediate cases. In

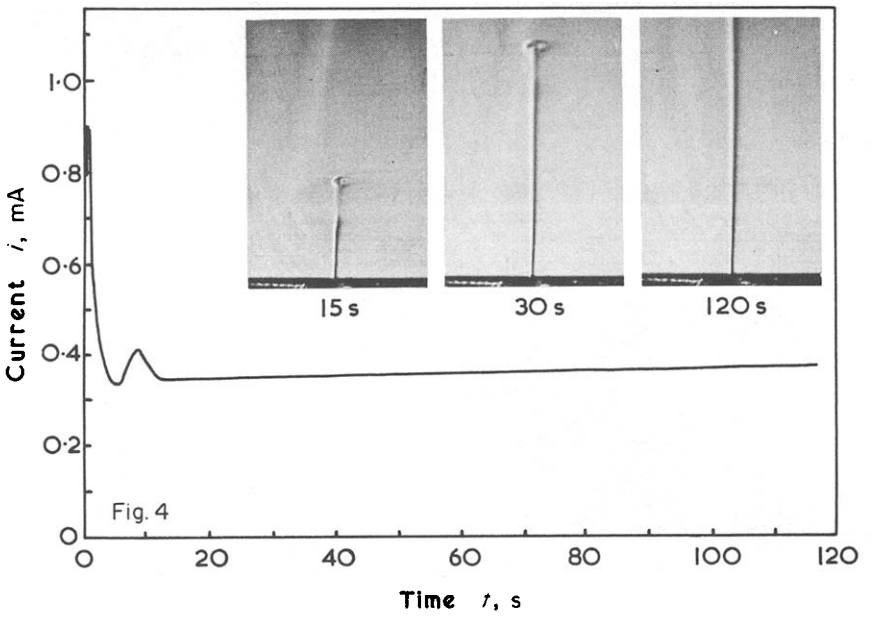

FIG. 4. Current–time plot and convection development for 1 mm electrode in 0·3 M solution, $Ra_d = 6{\cdot}43 \times 10^5$.

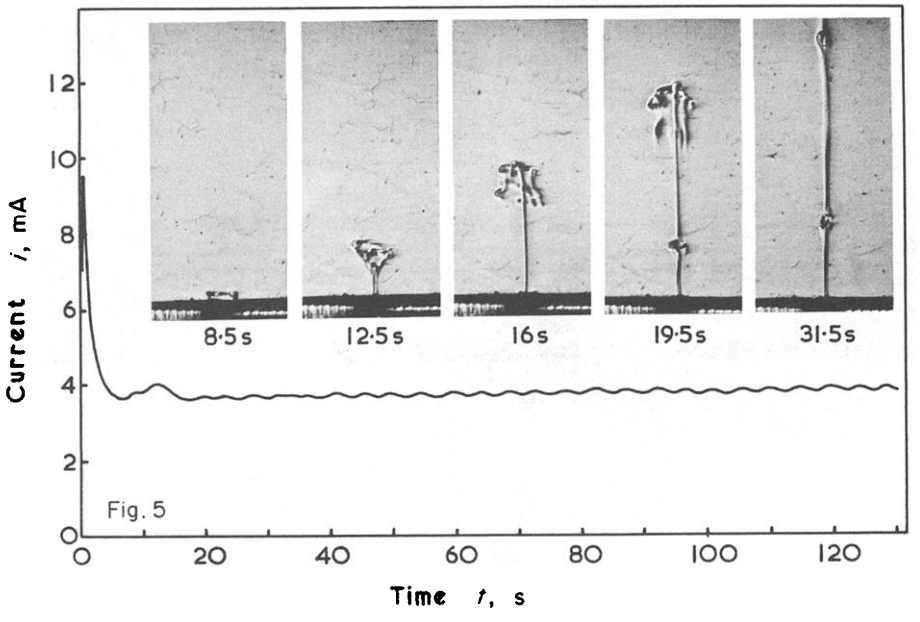

FIG. 5. Current–time plot and convection development for 2·5 mm electrode in 0·3 M solution, $Ra_d = 1{\cdot}0 \times 10^7$.

Fig. 5, which is for the 2·5 mm electrode in 0·3M solution, the electrode is now too wide to sustain a stable boundary layer to plume flow and there is a characteristic periodic instability within the mainly laminar plume which however, remains single. Initial lift-off instability is over the whole surface, $t = 8{\cdot}5$ s, and the flow quickly necks, $t = 12{\cdot}5$, before another boundary-layer instability becomes apparent, $t = 16$ s, and a second eruption occurs, $t = 19{\cdot}5$ s. This process repeats at regular intervals of about 5 s and the plume always contains regularly spaced nodules. In consequence of this periodic hydrodynamic behaviour the mass-transfer rate never becomes truly constant at steady state but fluctuates in a regular manner with the same frequency as the visible flow eruptions as can be readily seen from the transient plot.

The second intermediate case is depicted in Fig. 6 for the 10 mm electrode in the 0·1M solution. Here the electrode is sufficiently wide to produce multiple convection stream generation but the necking effect is so marked as to eventually merge into a single plume before a second multi-generation of convections occurs, $t = 41$ s. Again this transient clearly shows convection onset before the undershoot minimum is reached. Another feature of this plot is the occurrence of a distinct second undershoot minimum following the necking, $t = 34$ s, of the first generation of convection streams. The second generation causes a second current

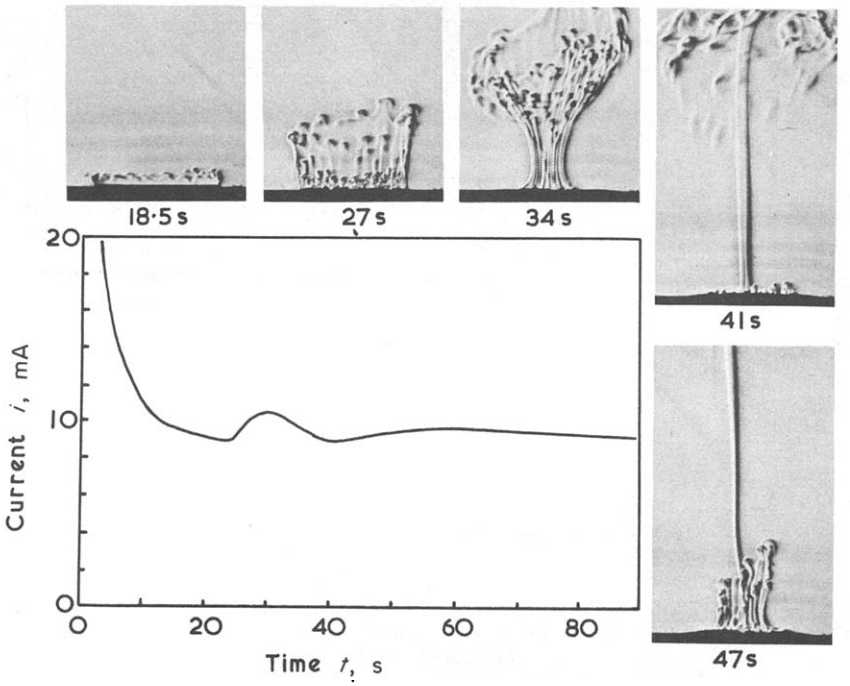

FIG. 6. Current–time plot and convection development for 10 mm electrode in 0·1 M solution, $Ra_d = 2{\cdot}16 \times 10^8$.

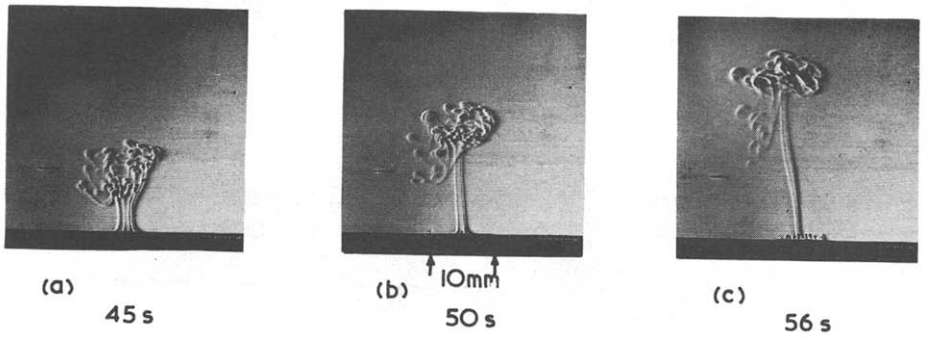

FIG. 7. Sequence showing boundary layer instability at 10 mm electrode in 0·05 M solution, $Ra_d = 1{\cdot}08 \times 10^8$.

rise, $t = 47$ s, before the system eventually settles to a steady state. The eruption of distinct generations of convection streams was clearly visible continually in this case at a period of 8·5 s.

The three photographs shown as Fig. 7 for the 10 mm electrode in 0·05 M $CuSO_4$ give a good illustration of the formation of a laminar boundary layer sweeping in over the electrode and feeding the central plume (b). Despite the fact that this is a moving layer and not a stagnant diffusion layer it periodically reaches an unstable thickness and begins to break up (c) into the multiplumed structure.

The present technique permits convenient observation of the effect of electrode roughening as deposition proceeds, especially in the more concentrated solutions. Figure 8 shows the result of a particularly interesting case of an extended run with conditions as for Fig. 4. A succession of plotter sweeps are shown with the time in minutes indicated. The flow remained

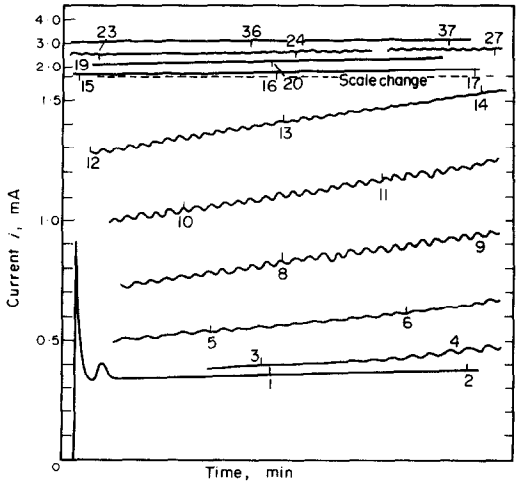

FIG. 8. Current–time plot for 1 mm electrode in 0·3 M solution showing long term effects of electrode roughening.

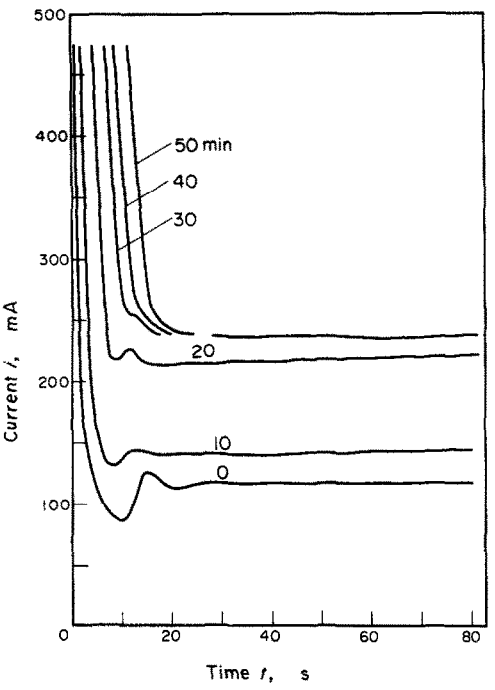

FIG. 9. Repeated transients at 20 mm electrode in 0·3 M solution. Cycle of 10 min active: 10 min dead.

laminar and the mass-transfer rate steady up to $t = 3\frac{1}{2}$ min when a regular fluctuation became apparent in the current with a corresponding periodic pulsation in the plume. This persisted until $t = 15$ min when the system reverted to a steady laminar flow, followed by a further later change to periodic fluctuation. The steep increase in the value of the limiting current is noteworthy, the value changing from 0·35 mA to 3·0 mA in 30 min, illustrating the difficulty of obtaining reproducible and meaningful results for mass transfer using electrodeposition techniques in situations leading to extreme electrode roughening.

The effect of electrode roughening is further illustrated in Fig. 9 where a repeated step potential change was applied at 20 min intervals with the 20 mm electrode in 0·03M solution. The system was active for 10 min and left switched off for 10 min before a further step was applied. A family of distinct and separate transients is produced, the effect of the large increase in surface area being particularly notable in the transient diffusion period as well as in the magnitude of the steady-state convective limiting current. The degree of undershoot is progressively diminished, and the tendency of the current to increase ceases at the longest times. At the end of this experiment a layer of powder some 0·75 mm thick had accumulated on the electrode.

The final electrodeposits on certain electrodes which had been active for a moderate length of time (≈ 20 min) were photographed and a typical resultant picture for $d = 20$ mm is shown in Fig. 10. A pattern of distinct radial striations is visible in the electrodeposit extending several mm inward from the circumference. The striations are probably caused by roll cells which remain positionally stable. The photographs of flow structure above a horizontal disk in heat transfer by Husar and Sparrow [8] show a very similar radial pattern.

DISCUSSION

(a) *Regimes of Flow*

It is clear from the current transients and corresponding photographs that a variety of flow structures can exist depending on plate size and electrolyte concentration. In Fig. 11 the four main flow types illustrated in Figs. 3–6 are related to the overall mass-transfer correlation previously established and the behaviour of all combinations of experimental conditions is included. Below a value of $Gr_d.Sc \approx 2 \times 10^5$ the flow has a simple single plumed laminar structure, (Fig. 4)

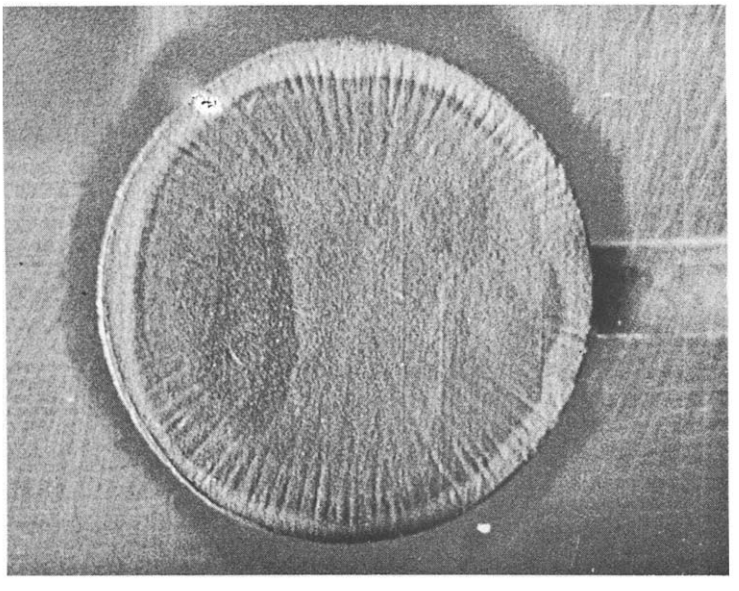

FIG. 10. Electrodeposit on 20 mm electrode.

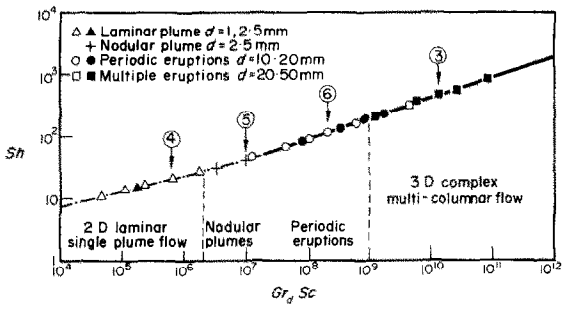

FIG. 11. Matching of flow regimes and correlation regimes in terms of surface Rayleigh number.

contrasting with the complex multi-columnar flow developed at $ScGr_d > 10^9$, (Fig. 3). Between these extremes as the value of $ScGr_d$ is increased the flow pattern takes on a progressively more multi-columnar form. Initially, small nodules interrupt the single laminar plume structure (Fig. 5). These appear to be caused by a periodic instability of the diffusion layer. The plate is becoming too wide to sustain a stable laminar flow. The nodules appear regularly at a time interval which decreases with increasing Rayleigh number. At higher values of $Gr_d.Sc(>10^8)$ the eruptions are multi-columnar and occur over much of the plate surface during the periodic disturbance (Fig. 6). As the Rayleigh number is further increased a continuous random generation of columns occurs ($Gr_d.Sc > 10^9$).

These regimes of flow behaviour give rise to a transition zone in the log–log plot of Sh against $Gr_d.Sc$. In the single laminar plume region the mass-transfer coefficient depends on plate diameter, in accordance with boundary-layer theory, whereas when the flow erupts in a multi-columnar form over the plate surface the effect of plate diameter on the mass-transfer coefficient is relatively unimportant as reflected by the 1/3rd exponent on the Rayleigh number in the correlation for this region.

(b) *Nature of current transients*

All the current transients determined for clean surfaces exhibited similar shapes. The initial decay of the current corresponds to simple diffusional thickening of a stable low density layer adjacent to the surface. Before the current had fallen to its minimum value optical observations showed a breakup of the simple diffusion layer. In the case of the larger surfaces the disturbance appeared to be initiated at the plate edges and spread inwards towards the centre.

Following Sparrow *et al.* [9] an attempt was made to estimate the value of the critical Rayleigh number ($Ra_{\delta,\mathrm{crit}}$) at which the initial conduction layer becomes unstable. This is given by:

$$Ra_{\delta,\mathrm{crit}} = \frac{\gamma g(c_\infty - c_0)\delta^3}{Dv}. \qquad (5)$$

Like Sparrow *et al.* δ was evaluated from

$$\delta = 2{\cdot}77\sqrt{(Dt_b)} \qquad (6)$$

where t_b is the layer break-up time observed optically.

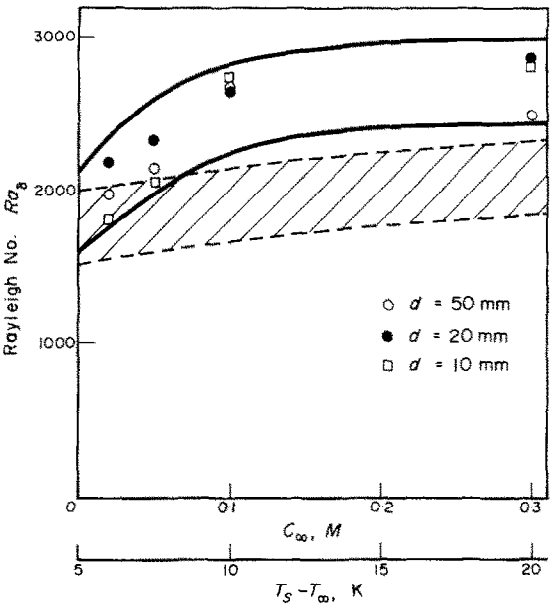

FIG. 12. Critical Rayleigh numbers for diffusion layer breakup (Ra_δ).

(This value of δ is obtained from the concentration distribution equation with $c/c_\infty = 0{\cdot}95$ at the edge of the diffusion layer.)

The values of Ra_δ calculated in this way are plotted in Fig. 12 against the solution concentrations for the larger electrodes. The shaded band represents the limits of Ra_δ from [9] obtained as a similar plot of Ra_δ vs $T_s - T_\infty$ for the heat-transfer periodic fluctuation case. The values of $Ra_{\delta,\mathrm{crit}}$ show similar scatter and the mean value is approximately 2400 as compared to the mean value of 1800 observed by Sparrow *et al.* This difference is to be expected since the present data are for initially stagnant conditions whereas Sparrow's correspond to the periodic generation of thermals where the solution must be in motion. Only data from the larger electrodes are considered since, at the smaller surfaces, edge effects lead to increasing departure from one dimensional diffusional conditions.

Figure 13 presents a correlation of the undershoot time (i.e. the time at which the current fell to its minimum value) for the full range of electrode diameters and solution concentrations tested. In this log–log plot

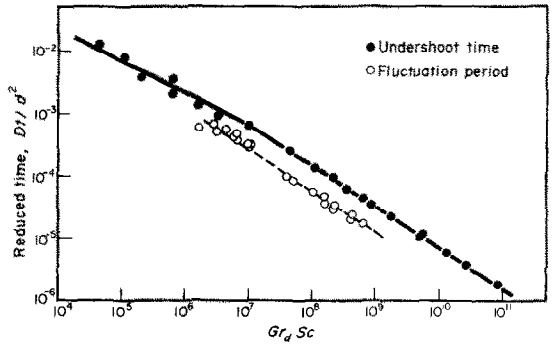

FIG. 13. Correlation of transient undershoot times and fluctuation periods in terms of Ra_d.

the undershoot time has been made non-dimensional by dividing by the mass diffusion time d^2/D. The data points fit the correlation line closely over the entire range of Rayleigh number and show the classic change of slope at $Ra \approx 10^7$ corresponding to the transition from single laminar plume flow. In the multi-columnar flow region the undershoot times correlate as:

$$\frac{Dt}{d^2} = 32{\cdot}5(Ra)^{-2/3} \tag{7}$$

thus since $Ra \propto d^3$, the undershoot time in this region is independent of electrode diameter. In the laminar plume regime the corresponding equation is:

$$\frac{Dt}{d^2} = 1{\cdot}80(Ra)^{-0{\cdot}51}. \tag{8}$$

Similar relations hold for the transient "overshoot" times except that these are of the order of 50 per cent greater than the undershoot times.

For those flows which went into regular oscillation following the transient diffusion regime, the fluctuation periods are also correlated on Fig. 13. The periods of these oscillations are seen to be considerably shorter than the layer break up times and the undershoot times, but they follow a consistently similar trend with Ra_d.

(c) *Laminar to "turbulent" transition*

Sections in standard heat-transfer texts (e.g. [17–21]) on thermal free convection from horizontal surfaces into unbounded fluids invariably present the two dimensionless equations

$$Nu = 0{\cdot}54Ra_d^{0{\cdot}25} \text{ for } 10^5 < Ra < 2 \times 10^7 \tag{9}$$

and

$$Nu = 0{\cdot}14Ra_d^{0{\cdot}33} \text{ for } 2 \times 10^7 < Ra < 3 \times 10^{10} \tag{10}$$

following the original work of Fishenden and Saunders [22]. Most authors speak of these equations applying to conditions of laminar and turbulent flow respectively with a transition Ra of 2×10^7. The present flow visualisation results suggest that this represents a considerable oversimplification of the transition criterion and that true turbulence is unlikely at values of Ra_d immediately above 2×10^7. Rather, the transition at a 1/3rd power on the Ra_d group is an indication that the transfer rate has become independent of the dimension of the transfer surface due to the establishment of a multi-columnar flow structure. The photographs of thermals rising from a heated surface presented by Sparrow *et al.* [9] do not indicate turbulence at Ra_d of the order of 10^8–10^9* and the mechanism of thermal generation as in the analogous mass-transfer case, is a regular periodic process in which only part of the cycle is a localised mixing following conduction layer detachment. This argument does not deny the possibility of turbulence at higher values of Ra and indeed when thermals become stronger and more closely spaced it is expected that the flow structure must inevitably become turbulent.

(d) *Electrode roughening*

With small electrodes and large concentrations a rapid roughening of the surface is apparent and this leads to the steep rises in current with time as illustrated in Fig. 8. This phenomenon creates problems in the measurement of mass transfer using the limiting electrolysis current technique for electrodeposition, since the plotting of current–voltage curves in order to locate the limiting current plateau usually takes 10–20 min during which time a considerable enhancement of current above the true smooth surface value must occur. The present transient technique offers a useful alternative approach to this problem. Several current–time transients may be recorded at different potential settings in order to determine limiting conditions. Then the steady convection region of the curve may be back extrapolated to $t = 0$ to give the mass-transfer rate which approximates closely to the true smooth surface value.

*The conditions under which the photographs of Fig. 2 of [9] were taken are not given and the above stated Rayleigh numbers are estimated from general information given in that paper.

REFERENCES

1. T. Mizushina, The electrochemical method in transport phenomena, *Adv. Heat Transfer* **7**, 87 (1971).
2. T. K. Ross and A. A. Wragg, Electrochemical mass transfer studies in annuli, *Electrochim. Acta* **10**, 1093 (1965).
3. J. R. Lloyd, E. M. Sparrow and E. R. G. Eckert, Laminar transition and turbulent natural convection adjacent to inclined and vertical surfaces, *Int. J. Heat Mass Transfer* **15**, 457 (1972).
4. A. A. Wragg, Free convection mass transfer at horizontal electrodes, *Electrochim. Acta* **13**, 2159 (1968).
5. A. A. Wragg and R. P. Loomba, Free convection flow patterns at horizontal surfaces with ionic mass transfer, *Int. J. Heat Mass Transfer* **13**, 439 (1970).
6. E. E. Soehngen, Experimental studies on heat transfer at very high Prandtl numbers, in *Progress in Heat and Mass Transfer*, Vol. 2, p. 125. Pergamon Press, Oxford (1969).
7. C. M. Vest and M. L. Lawson, Onset of convection near a suddenly heated horizontal wire, *Int. J. Heat Mass Transfer* **15**, 1280 (1972).
8. R. B. Husar and E. M. Sparrow, Patterns of free convection flow adjacent to horizontal heated surfaces, *Int. J. Heat Mass Transfer* **11**, 1206 (1968).
9. E. M. Sparrow, R. B. Husar and R. J. Goldstein, Observations and other characteristics of thermals, *J. Fluid Mech.* **41**(4), 793 (1970).
10. Z. Rotem and L. Claassen, Free convection boundary layer flow over horizontal plates and discs, *Can. J. Chem. Engng* **47**, 461 (1969).
11. Z. Rotem and L. Claassen, Natural convection above unconfined horizontal surfaces, *J. Fluid Mech.* **39**(1), 173 (1969).
12. A. A. Wragg and A. K. Nasiruddin, Ionic mass transfer by free convection with simultaneous heat transfer, *Electrochim. Acta* **18**, 619 (1973).
13. L. N. Howard, Convection at high Rayleigh number, in *Proc. 11th Int. Cong. Appl. Mech.* (edited by H. Gortler). Springer, Berlin (1969).
14. M. Eisenberg, C. W. Tobias and C. R. Wilke, Selected properties of ternary electrolytes employed in ionic mass transfer studies, *J. Electrochem. Soc.* **103**, 413 (1956).

15. A. J. Arvia, J. C. Bazan and J. S. W. Carrozza, Electrochemical study of the diffusion of cupric ion in aqueous and aqueous-glycerol solutions containing sulphuric acid, *Electrochim. Acta* **11**, 881 (1966).
16. C. R. Wilke, M. Eisenberg and C. W. Tobias, Correlation of limiting currents under free convection conditions, *J. Electrochem. Soc.* **100**, 513 (1953).
17. F. Kreith, *Principles of Heat Transfer*, 3rd edn. International, London (1965).
18. A. J. Chapman, *Heat Transfer*, 3rd edn. Macmillan, New York (1974).
19. W. H. McAdams, *Heat Transmission*, 3rd edn. McGraw-Hill, New York (1954).
20. A. J. Ede, *Introduction to Heat Transfer Principles and Calculations*. Pergamon, Oxford (1967).
21. F. J. Bayley, J. M. Owen and A. B. Turner, *Heat Transfer*. Nelson, London (1972).
22. M. Fishenden and O. A. Saunders, *An Introduction to Heat Transfer*. Oxford, New York (1950).

ETUDES OPTIQUES ET ELECTROCHIMIQUES DU TRANSFERT DE MASSE EN CONVECTION LIBRE TRANSITOIRE SUR DES SURFACES HORIZONTALES

Résumé—Le déclenchement de la convection libre sur des surfaces horizontales adjacentes à une ambiance de fluide libre située au-dessus a été étudié à l'aide d'un système électrochimique basé sur le dépôt d'ions Cu^{2+}. Une technique de variation étagée du potentiel est employée et la photographie du développement, qui s'ensuit, de structures convectives a été synchronisée avec l'enregistrement des variations du courant électrique. Cela a permis de visualiser l'interdépendance entre le taux de transfert massique instantané et la structure de l'écoulement convectif. Un certain nombre de structures distinctes d'écoulement dans les régimes instationnaire et stationnaire a été observé et elles ont été reliées aux régimes des domaines de corrélation pour le transfert massique global. Des phénomènes intéressants faisant intervenir des instabilités périodiques ont été découverts pour des nombres de Rayleigh de transition conduisant à des pulsations dans le sillage convectif et à des oscillations régulières analogues dans le taux de transfert de masse à l'état stationnaire.

L'effet des rugosités de surface sur le transfert de masse et sur le régime hydrodynamique a été observé lors d'expériences prolongées et une méthode est suggérée afin d'éviter les difficultés d'application de la méthode électrochimique dûes à la présence de rugosités de surface.

Les temps de diffusion transitoires par défaut sont corrélés au nombre de Rayleigh de la plaque par les équations

$$\frac{Dt}{d^2} = 32{,}5(Gr_d . Sc)^{-2/3}$$

dans la zone $10^7 < Ra_d < 10^{11}$ et

$$\frac{Dt}{d^2} = 1{,}80(Gr_d . Sc)^{-0{,}51}$$

dans la zone $10^4 < Ra_d < 10^7$

De même, les fréquences des fluctuations périodiques sont corrélées par l'équation:

$$\frac{Dt}{d^2} = 12{,}8(Gr_d . Sc)^{-2/3}.$$

OPTISCHE UND ELEKTROCHEMISCHE UNTERSUCHUNGEN DES INSTATIONÄREN STOFFÜBERGANGS BEI FREIER KONVEKTION AN HORIZONTALEN OBERFLÄCHEN

Zusammenfassung—Das Einsetzen der freien Konvektion über einer horizontalen Oberfläche in einem ruhenden Fluid wurde mit Hilfe eines elektrochemischen Verfahrens, das auf der galvanischen Ablagerung von Cu^{++}-Ionen beruht, untersucht. Eine instationäre Potential-Schritt-Technik wurde angewandt, und es wurden Fotos der sich ausbildenden konvektiven Strukturen den Aufzeichnungen der Strom-Zeit-Übergangsverläufe zugeordnet. So konnte der Zusammenhang zwischen augenblicklichem Stoffübergangsstrom und konvektiver Strömungsform aufgezeigt werden. Eine Anzahl unterschiedlicher Strömungsformen wurde im instationären und stationären Fall beobachtet und den Korrelationsbereichen für den Gesamtmassenstrom zugeordnet. Bei Rayleigh-Zahlen des Übergangsbereichs wurden interessante Phänomene entdeckt. Dort treten periodische Instabilitäten auf, die zu Pulsationen in der Konvektionsströmung und entsprechenden regelmäßigen Schwankungen in der stationären Stoffübergangsmenge führen.

In Langzeitversuchen wurde der Einfluß der Aufrauhung der Oberflächen auf Stoffübergang und Strömungsform untersucht. Die Autoren schlagen eine Methode vor, mit der die durch die Oberflächenaufrauhung bei der Anwendung elektrochemischer Techniken bedingten Schwierigkeiten bewältigt

werden können. Die Übergangszeit der Diffusion ist mit der Platten–Rayleigh–Zahl verknüpft durch die Gleichungen

$$\frac{Dt}{d^2} = 32{,}5(Gr_d . Sc)^{-2/3}$$

im Bereich $10^7 < Ra_d < 10^{11}$ und

$$\frac{Dt}{d^2} = 1{,}80(Gr_d Sc)^{-0{,}51}$$

im Bereich $10^4 < Ra_d < 10^7$. Für die periodischen Schwankungsfrequenzen gilt

$$\frac{Dt}{d^2} = 12{,}8(Gr_d Sc)^{-2/3}$$

ИССЛЕДОВАНИЕ НЕСТАЦИОНАРНОГО МАССОПЕРЕНОСА ПРИ СВОБОДНОЙ КОНВЕКЦИИ НА ГОРИЗОНТАЛЬНЫХ ПОВЕРХНОСТЯХ С ИСПОЛЬЗОВАНИЕМ ОПТИЧЕСКИХ И ЭЛЕКТРОХИМИЧЕСКИХ МЕТОДОВ

Аннотация — В работе электрохимическим способом (электролитическое осаждение ионов Cu^{2+}) изучается возникновение свободной конвекции на горизонтальных поверхностях, обращенных вверх и граничащих с жидкой средой. Использована методика переменного потенциала, а фотографирование наблюдаемой картины развивающейся конвективной структуры было синхронизировано с записью изменения тока в зависимости от времени. Это позволило определить взаимосвязь между мгновенной скоростью масообмена и структурой конвективного потока. Изучено большое количество характерных конвективных структур в нестационарных и стационарных условиях, которые были связаны с зависимостями для суммарной скорости массообмена. Были обнаружены интересные явления, включающие колебательную неустойчивость при переходных числах Релея, которые приводят к пульсациям в конвективных струйках и к соответствующим колебаниям скорости массопереноса при стационарных условиях.

В процессе эксперимента определено влияние шероховатости поверхности на массообмен и гидродинамику.

Предлагается способ устранения трудностей в применении электрохимического метода, обусловленных шероховатостью поверхности.

Время уменьшения диффузии в нестационарных условиях описывается уравнениями с использованием числа Релея для пластины

$$\frac{Dt}{d^2} = 32{,}5(Gr_d Sc)^{-2/3}$$

в диапазоне $10^7 < Re_d < 10^{11}$

$$\frac{Dt}{d^2} = 1{,}80(Gr_d Sc)^{-0{,}51}$$

в диапазоне $10^4 < Ra_d < 10^7$.

Частота периодических колебаний описывается подобным же образом уравнением

$$\frac{Dt}{d^2} = 12{,}8(Gr_d Sc)^{-2/3}.$$